

31 5-806

THE FRANKLIN INSTITUTE • Laboratories for Research and Development
Quarterly Progress Report No. P-2236-8

AD No. 21995
ASTIA FILE COPY

PERMANENT MAGNET MATERIALS

October 1, 1952 to December 31, 1952

Prepared for
Chief of Naval Research, Department of the Navy
Under Contract No. Nonr-01002

FILE COPY
NAVY RESEARCH SECTION
SCIENCE DIVISION
LIBRARY OF CONGRESS
TO BE RETURNED

Approved by:

Foster C. Nix
Foster C. Nix
Associate Director

Approved by:

Nicholas H. Smith
Nicholas H. Smith
Director

Copy No. 2

DISTRIBUTION LIST
(Quarterly Status)

Copy
Number

- 1 - 3 Chief of Naval Research
Department of the Navy
Washington 25, D. C.

Attention: Physics Branch
- 4 Office of Naval Research, New York
346 Broadway
New York, New York

Attention: Mr. Irving Rowe
- 5 Resident Representative
Office of Naval Research
c/o University of Pennsylvania
3320 Walnut Street
Philadelphia 4, Pennsylvania

Attention: Mr. S. Serraris
- 6 Ordnance Research Laboratory
State College, Pennsylvania

TABLE OF CONTENTS

	<u>Page</u>
ABSTRACT	v
1. INTRODUCTION	1
1.1 Choice of Methods of Particle Size Determination	1
1.2 Description of Powders Studied	3
2. DETAILED DESCRIPTION OF THE METHODS	4
2.1 Electron Microscope	4
2.1.1 Preparation of Samples	5
2.1.2 Calibration of Microscope	10
2.1.3 Errors	13
2.2 X-Ray Diffraction	13
2.2.1 Apparatus	13
2.2.2 Method	14
2.2.3 Relation of X-ray to Electron Microscope Sizes	21
2.2.4 Errors, etc.	22
2.3 Surface Areas Measurements by the Nitrogen Adsorption Technique	24
2.3.1 Method	24
2.3.2 Apparatus	26
2.3.3 Conditions of Measurement	28
2.3.4 Measurement Procedure	30
2.3.5 Errors	33
2.3.6 Relation of N ₂ Adsorption to Electron Microscope Diameters	36

TABLE OF CONTENTS (Cont'd)

	<u>Page</u>
2.4 True Powder Density	37
3. CONCLUSION	37
3.1 Results	37
3.2 Discussion	38

LIST OF TABLES

<u>Table</u>	<u>Page</u>
1-1 Powders Used in This Study	3
2-1 Comparison of X-ray and Electron Microscope Sizes	23
2-2 Comparison of Warren, Jones, and Stokes Particle Sizes	24
2-3 Reproducibility of Surface Area Measurements	34

LIST OF FIGURES

<u>Figure</u>	<u>Page</u>
2-1 Frequency Dependence of μ_r, μ_i For Magnetic Particle Dispersion	8
2-2 Electron Micrographs	11
2-3 Electron Micrographs	12
2-4 Nitrogen Adsorption Apparatus	27
2-5 Outgassing Temperature ($^{\circ}\text{C}$)	29
3-1 Comparison of Measurements of Iron Powders	39

ABSTRACT

An experimental comparison has been made of the particle sizes of single domain ferromagnetic powders determined with three independent methods. The methods used the electron microscope, the broadening of X-ray diffraction lines, and the measurement of surface areas with nitrogen adsorption.

A method of preparing electron microscope specimens with reasonable separation of single-domain particles is described.

Good agreement was obtained between the electron microscope and the X-ray methods, but the nitrogen adsorption values were consistently higher. These results have been interpreted as support of the validity of the particle size distributions determined with the electron microscope.

1. INTRODUCTION

The Franklin Institute Laboratories, under this contract, are studying the magnetic properties of very fine ferromagnetic powders. One of the most important experimental tasks in this project is the determination of the particle size distribution of these powders, which range from 100 Angstroms to one micron (10,000 Angstroms). A study of possible methods was made, and is reported here.

1.1 Choice of Methods of Particle Size Determination

The better known methods for determining particle size, such as sieving, sedimentation, elutriation, etc., were not applicable to these powders. Sieving could not be used because wire mesh cannot be produced uniformly with a hole size less than about 40 microns. Any method using suspensions of the particles in liquids would also be useless because the strong magnetic interactions between the small particles makes them clump, and what would actually be measured is the clump size. This would also be true for all sedimentation methods, both in liquid and vapor phase, for air elutriation, centrifuging, and the turbidity and optical density methods. The resolving power of the ordinary microscope at its very best is limited to values greater than about 0.2 microns, and could be used only in the upper range of the particle sizes of interest here.

Because the standard methods of particle size measurement were of no value in this study, it was decided to choose methods which, although

not so well-known, were applicable to these particles. The task then was to study the methods themselves, to compare the results given by each for agreement among them, and in general to investigate their reliability. This report contains a summary of this study.

Three methods were chosen. The electron microscope, with resolution between one micron and 50 Angstroms, was selected as the central method. With this instrument it was possible to obtain the complete particle size distribution. In order, however, to be sure that all the particles in the sample were counted, and that the sample chosen was a representative one, the electron microscope results were checked by two other methods. These were the broadening of X-ray diffraction lines, and the determination of total surface area by the BET (Brunauer, Emmett and Teller)¹ nitrogen adsorption method. The broadening of the X-ray diffraction lines can be interpreted to give a measure of the average crystallite size in the range from 100 to 500 Angstroms. This crystallite size is equal to or smaller than the actual particle size. The method has the tremendous advantage with these magnetic powders in that it is not sensitive to the clumping of the particles. The BET method, which gives the total surface area of a sample, is useful in the range of particle sizes less than one micron. From the total surface area an average particle size may be calculated. The BET method is also not very sensitive to clumping.

As will be shown later in this report, the average particle size to be expected from both the X-ray diffraction line broadening and from the BET method could be calculated from the particle size distribution

as obtained with the electron microscope, making only the assumption that the particles were spherical. A comparison among these methods was made by calculating each of these averages from the electron microscope distribution, and comparing them with the averages obtained by the two subsidiary methods. The nature of the agreement obtained can be taken as a measure of the validity of the distributions as determined with the electron microscope.

1.2 Description of Powders Studied

The following table presents a list of the powders used in this investigation:

Table 1-1 - Powders Used in This Study

<u>Designation</u>	<u>Approx. Particle Size</u>	<u>% Free Metal</u>
GAF "HP"	5 μ	99
GAF "P-818"	2 μ	98
Fe-8	600 \AA	87
Fe-7	400 \AA	69
Hyflux	400 \AA	90
NOL-1	250 \AA	79
NOL-2	200 \AA	40
Ugine	200 \AA	58

The two powders labelled GAF were carbonyl Fe, produced by the General Aniline and Film Corporation. "HP" was one of the commercial products, while "P-818" was an experimental run in a smaller particle size range than is usually produced commercially. We wish to acknowledge the generosity of

Dr. Hans Beller, of General Aniline, for supplying us with the P-818 and also the Ugine powder, described below. NOL-1 was produced by the reduction of Fe formate, in the Magnetics Laboratory at the Naval Ordnance Laboratory. Hyflux was made by the Raney process, and was given to us through the courtesy of the Indiana Steel Products Company. All of the above powders were Fe base. The other two, Ugine and NOL-2, were an Fe-Co alloy. Both were made by formate reduction, the Ugine by the Societe d'Electro-Chimie, d'Electro Metallurgie et des Acieries Electrique d'Ugine, and NOL-2 by the Magnetics Laboratory at NOL.

2. DETAILED DESCRIPTION OF THE METHODS

2.1 Electron Microscope

Provided that the sample chosen and presented in the field of the electron microscope is representative of the powder under study, and provided that the individual particles are separated enough so that they may be distinguished, an accurately calibrated electron microscope should give a completely reliable particle size distribution. The only check upon the representative quality of the sample, other than an intercomparison of the results of different methods such as is presented in this report, lies in the repeated determination of particle size distribution from different samples of the powder. With ordinary, non-magnetic powders, dispersion of the particles often proves to be a problem. With the magnetic powders considered in this report, the dispersion problem is even more severe.

2.1.1 Preparation of Samples

Initial attempts to prepare samples for the electron microscope using standard methods were successful only with the powders whose particle size was of the order of 400 Å or larger. These samples were prepared by transferring the powder, either dry or while suspended in benzene, to a high carbon steel mortar and pestle. A 2 percent collodion solution in amyl acetate was added to the powder to make a paste. The paste was then mullied over a prolonged period of time, amyl acetate being added periodically to replace that lost by evaporation. During this mulling process any benzene present in the powder also evaporated. The resulting suspension was then spread onto a glass microscope slide to form a smooth film, and a portion of the film transferred with scotch tape to a copper specimen screen. Blanks were also prepared in an identical fashion, but without the powder present, in order to account for any contamination picked up during the mulling operation. This technique was successful with the HP, P818, Hyflux, Fe-8 and Fe-7 powders, but failed completely to give reasonable dispersions with the finer powders.

For these smaller powders, the mulling technique was tried with formvar as well as with collodion, using a glass plate with a spatula as well as with a mortar and pestle, and by ball - milling. A number of wetting agents and different solvents were also tried, all with a conspicuous lack of success in separating the powders.

Successful micrographs of these powders were finally obtained by putting the collodion suspensions in a fairly intense alternating magnetic

field, instead of using the standard mulling. These suspensions were prepared from approximately 10 mg of powder added to 0.3 cc of a 5 percent collodion solution in amyl acetate. This mixture was put into a small gelatin capsule together with a glass ball. The capsule was then inserted in a gap cut in an ordinary filter choke, through which sufficient 60 cycle a-c current was passed to produce a field strength of approximately 1800 Oersteds rms. These chokes were mounted on a rocking platform in such a way that the glass ball rolled from end to end in the capsule, adding mechanical mixing to the effect of the magnetic field. This process was allowed to continue for about a week, when the contents of the capsule were emptied onto a glass slide, and the collodion diluted to give a film of the proper thickness. The actual film was formed by squeezing the suspension between two glass slides and then was picked up on a specimen screen as before. The concentration of powder was chosen so as to give an adequate coverage of the field of view of the microscope. Experience showed that the collodion solution had to be quite viscous. The 5 percent solution actually used was the most viscous solution easily prepared.

The action of the magnetic field in dispersing the powders can be understood from the following considerations. The suspension is a system possessing a magnetic permeability, derived from the presence of the ferromagnetic particles. In this small particle size range, the individual particles are predominantly single domain and therefore react to the magnetic field as individual dipoles. At sufficiently low frequencies, these particles experience no difficulty in following the reversals of the alternating

field, and the permeability of the mixture is high. If the frequency of oscillation of the magnetic field be made high enough, however, the particles, due to the viscous drag imposed by the solvent, can no longer follow the field and the permeability is reduced to some low value. Such a behavior can be represented mathematically, using the usual complex notation for the magnetic field, by writing the permeability as a complex number

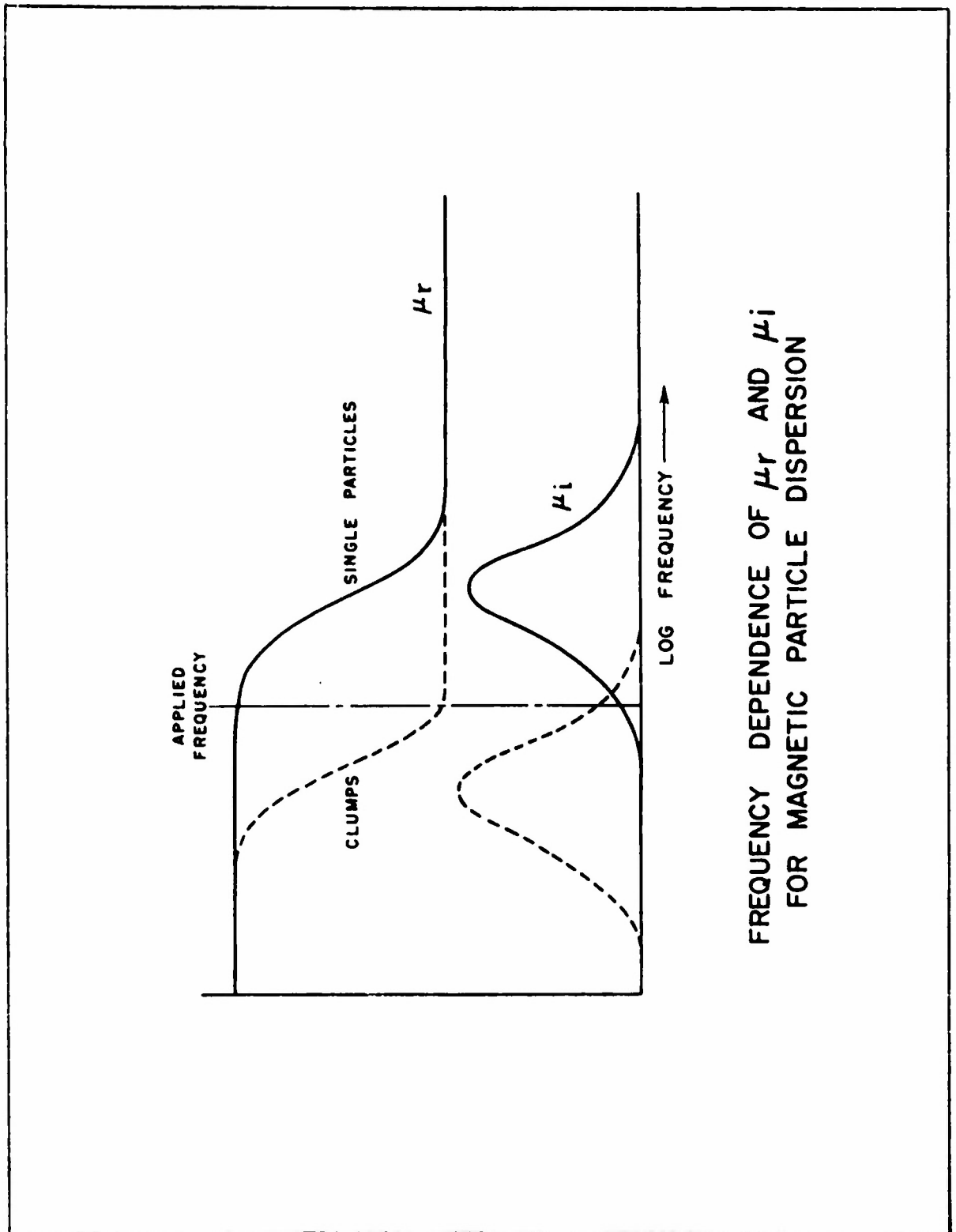
$$\mu^* = \mu_r + i\mu_i$$

in which μ_r represents the in-phase component of the reaction of the material to the field, and μ_i the out-of-phase component of the reaction. The energy stored per cycle in the material is given by

$$E = \frac{\mu_r \overline{H^2}}{8\pi},$$

where $\overline{H^2}$ is the mean square magnetic field strength. A dispersion subjected to a field of constant frequency in a medium of a given viscosity will tend to produce the maximum energy stored, which implies a maximum μ_r .

For a given particle size, the behavior of μ_r and μ_i with frequency should be of the type described by Debye² for the behavior of the real and imaginary parts of the complex dielectric constant for polar molecules. This variation with frequency is illustrated in Figure 2-1. The critical frequency, when μ_i rises to a maximum and μ_r begins to drop, depends upon particle size and solvent viscosity. At frequencies less



FREQUENCY DEPENDENCE OF μ_r AND μ_i
FOR MAGNETIC PARTICLE DISPERSION

than the critical frequency, μ_r is large because of the orientation of the particles; while at frequencies higher than the critical frequency, orientation cannot occur and μ_r is low. Debye² has given an equation relating this critical frequency to the solvent viscosity and the particle size for spherical particles:

$$f_c = \frac{kT}{8\pi^2\eta a^3} \quad (2.1)$$

in which f_c is the critical frequency, η is the solvent viscosity given in poises, a is the radius of the particle in cm., k is Boltzmann's constant, and T is the absolute temperature.

For a suspension composed of clumps of particles, the clumps may be treated like ordinary particles. That is, according to equation (2.1) the large clumps will have large values of "a" and therefore low critical frequencies. If the frequency of the applied field and the viscosity be chosen such that the critical frequency for a single particle is slightly higher than the applied frequency (see Fig. 2-1), then the critical frequencies for even the smallest clumps will be less than the applied frequency. This means that only single particles will be able to orient with the field, and that in the presence of the field, μ_r can increase if the clumps break up into single particles, thereby freeing the particles to orient. Since this increase in μ_r will result in an increase in the stored energy, there will be a tendency for dispersion to

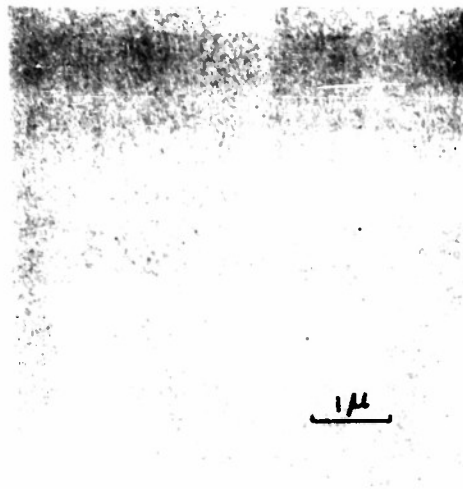
take place.

With Debye's² equation (2.1), it should be possible to calculate the value of the viscosity required for an applied frequency of 60 cps and a single particle diameter of approximately 300 Angstroms. The calculated value at 25°C is about 3 poises, which represents a very viscous solution. On this basis it is understandable why the most viscous solution possible has proven to be the most successful.

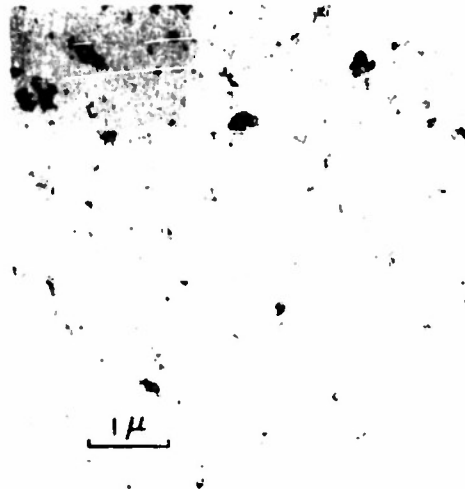
A comparison between the dispersions obtained with some of the finer powders, using this method and the standard mulling methods, is shown in Figures 2-2 and 2-3. The magnetic method gives much better dispersion, so much so that individual particles are clearly defined. The lower magnification micrograph of the Uguine powder is included to show a larger part of the field of view. Some clumps persist with a definite tendency to form chains.

2.1.2 Calibration of Microscope

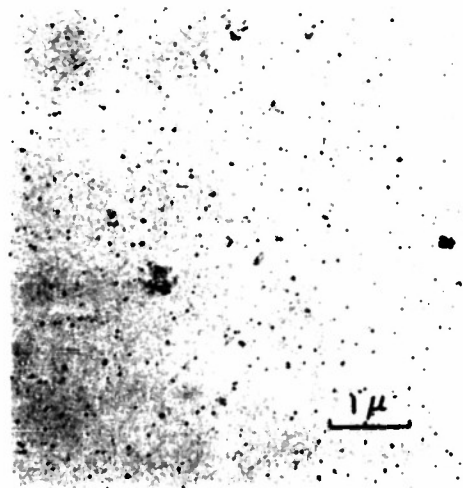
To determine the size of a particle shown in a micrograph, the instrument must be calibrated. In this case calibration was done using a replica of a Johns-Hopkins' grating with 15,000 lines per inch. Such replicas are stated to be accurate to within 3%.³ Care was taken to choose replicas which showed no distorted patterns. To get reproducible conditions of magnification it was necessary to saturate the pole pieces of the objective and projection lenses. This was done by turning the current in these lenses on and off at 30-second intervals, allowing them to come to



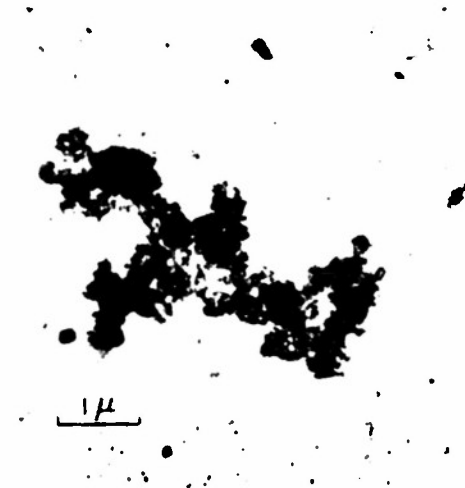
(A) BLANK FOR MAGNETIC DISPERSION
(10,400X)



(B) UGINE POWDER, MAGNETIC DISPERSION
(10,400X)

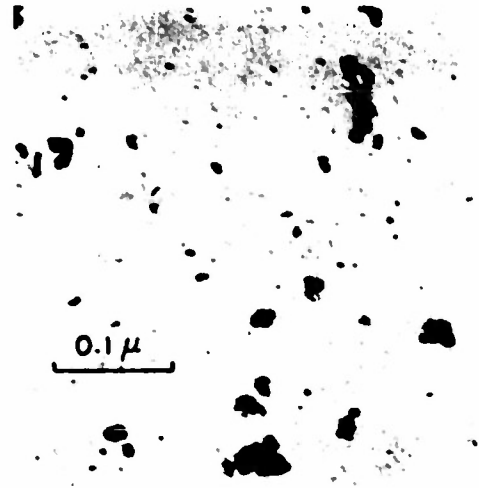


(C) BLANK FOR HAND MULLING
(10,400X)



(D) UGINE POWDER, HAND MULLED
(10,400X)

ELECTRON MICROGRAPHS
(BLANKS, UGINE POWDERS)



(A) UGINE POWDER, MAGNETIC DISPERSION
(158,000X)



(B) NOL POWDER, MAGNETIC DISPERSION
(158,000X)



(C) HYFLUX POWDER, HAND MULLED
(32,600X)

ELECTRON MICROGRAPHS
(UGINE, NOL, HYFLUX POWDERS)

equilibrium. The objective was refocussed each time it was on. In general, each lens required at least six such alternations. During the calibration, about four pictures were taken at each magnification from different replicas, and ten measurements were taken from each picture. Any systematic variations, if excessive, were investigated. In most cases these variations were found to be due to unsaturated pole pieces, and were corrected when the pole pieces were saturated.

2.1.3 Errors

Total probable error in the measurements was calculated by taking into account the following terms:

- (1) Replica error, 3%;
- (2) Direct measurement on photograph, 4%;
- (3) Deviations due to variations in saturation of pole pieces, and uniform expansion or contraction of the replicas, 4%.

The total probable error is then of the order of 7%. Another possible source of error has not been taken into account. There may be distortion of the electron beam because of the magnetic fields produced by the single domain particles. Meiklejohn and Paine⁴ have shown, however, that the effect on both particle size and shape is probably negligible.

2.2 X-Ray Diffraction

2.2.1 Apparatus

The apparatus used in the determination of particle size was a

General Electric X-ray Spectrometer, XRD-3. The Geiger counter of the spectrometer was set at predetermined angles, and counts taken manually. An Fe tube with Mn filter was used for all of the measurements, with a wave length of 1.934 Angstroms.

2.2.2 Method

X-ray diffraction lines are in general broadened due to four factors.⁵ A certain amount of breadth is always inherent in the apparatus. In addition the diffraction lines may be further broadened due to the effect of small particles, of lattice distortion, or of stacking faults. Warren and Averbach⁶ have shown that it is possible to separate the broadening due to the last three causes. Their technique, however, involves obtaining diffraction lines of higher orders. With the equipment used in the present study, the intensity of the signal was not sufficiently high above the background to obtain more than the three strongest lines in the Fe spectrum, at values of 2θ equal to 57° , 81° and 111° , and these are not suitable for the technique of Warren and Averbach. For this reason, it is not possible to state definitely that the broadening observed was due solely to the effect of particle size. However, because of the methods used in preparation with these powders, the presence of strain or stacking faults seem unlikely; thus the assumption is made that all broadening was due to particle size. The broadening of the 57° line in all cases was used. For the Ugine and NOL-2, which were 70:30 FeCo alloys, the lattice structure is b.c.c., with the same parameter as α -Fe to within 0.1%.⁷

The average particle diameter can be calculated using the Scherrer equation (see, for instance, James⁸)

$$d_{\beta} = \frac{K\lambda}{\beta \cos\theta}$$

in which K equals the shape factor, λ is the wave length, θ is the Bragg angle, and β the breadth of the diffraction line due to the particle size, measured in units of 2θ (radians). The value for K is in doubt to about 20 percent, depending upon particle shape and crystal form (Jones⁹). A value of K equal to 0.94 was used in this work.

The value for β in the equation must be that due solely to the particle size, and must be obtained from the observed breadth of the diffraction line after correction for instrumental broadening. Alexander¹⁰ has shown that for a linear absorption coefficient > 40 , and $2\theta \geq 20^\circ$, the only important sources of instrumental broadening are the X-ray source and receiver widths, and the $\alpha_1 - \alpha_2$ doublets. For Fe, the linear adsorption coefficient is 350 (International Critical Tables), and 2θ for the most important diffraction line is 57° . The work reported here, therefore, meets both the initial conditions. The resolution of the equipment used was such that the $\alpha_1 - \alpha_2$ doublet could not be resolved.

Numerous methods have been proposed for correcting the observed line for instrumental broadening effects. Warren⁵ proposed use of an equation, valid if all line profiles are strictly Gaussian

$$\beta^2 = B^2 - b^2$$

in which β is the line breadth due purely to particle size, B the observed breadth, and b the instrumental breadth. The latter is the breadth of the same diffraction line of a sample with crystallites too large to cause any broadening. Jones⁹ has given correction curves based upon semi-empirical procedures. Recently, Stokes¹¹ has shown how to make a rigorous correction using a Fourier analysis technique. Because the use of Patterson-Tunell¹² strips makes these numerical computations relatively simple, it was decided to use this rigorous method. There are not too many accounts of the actual procedure to be found in the literature; therefore, a rather detailed description will be given here.

According to Stokes¹¹, the instrumental, observed, and pure particle size profiles may be represented, respectively, by

$$g(x) = \sum_{-\infty}^{+\infty} G(n) e^{-i \frac{2\pi n x}{a}}$$

$$h(x) = \sum_{-\infty}^{+\infty} H(n) e^{-i \frac{2\pi n x}{a}}$$

$$f(x) = \sum_{-\infty}^{+\infty} F(n) e^{-i \frac{2\pi n x}{a}}$$

in which x , the Bragg angle, is the abscissa of the profiles, and runs from $-a/2$ to $+a/2$. Then the particle size profile can be determined from the other two, because

$$F(n) = \frac{1}{a} \frac{H(n)}{G(n)}$$

Since these quantities are complex, the real and imaginary parts must be calculated separately. The $1/a$ factor may be neglected.

The problem of determining the line profile due to the sample is reduced to that of expressing the instrumental and observed lines in terms of their Fourier coefficients. This may readily be done using the Patterson-Tunell strips. We will consider one line, for instance, the observed broad line, $h(x)$. The Fourier coefficients are given by

$$H_r(n) = \frac{1}{a} \int_{-a/2}^{a/2} h(x) \cos\left(\frac{2\pi nx}{a}\right) dx$$

Real Part

$$H_i(n) = \frac{1}{a} \int_{-a/2}^{a/2} h(x) \sin\left(\frac{2\pi nx}{a}\right) dx$$

Imaginary Part

The interval $-a/2$ to $+a/2$ along the abscissa may be divided into N units, and the integrals replaced by sums over these intervals, (Stokes has given the conditions under which this is legitimate) using the substitution $x/a = X/N$

$$H_r(n) = \frac{1}{N} \sum_{-N/2}^{N/2} h(X) \cos\left(\frac{2\pi nX}{N}\right) \text{ etc.}$$

Since $\text{Cos}(\phi) = \text{Cos}(-\phi)$ and $\text{Sin}(\phi) = -\text{Sin}(-\phi)$, and with $N = 60$, $h(X) + h(-X) = h'(X)$, and $h(X) - h(-X) = h''(X)$, the sums may be simplified to

$$H_r(n) = \frac{h(0)}{N} + \sum_1^{N/2} h'(X) \cos(nX6^\circ) \tag{2.2}$$

$$H_i(n) = \sum_1^{N/2} h''(X) \sin(nX6^\circ)$$

Both n and X are integers, so that nX is an integer. Further, the only independent quantities involved are the values for the $\text{Cos } nX 6^\circ$ for which nX has integral values from 1 to 15. Each strip corresponds to a given value for h' (or h''), the amplitude, and contains these 15 values for $h' \text{ Cos } nX 6^\circ$. When the 30 strips, one for each $h'(X)$ with X from 1 to 30, are arranged in order, they form a complete table containing all the numbers required to

form the sums in equations (2.2). All that is needed is to choose the proper numbers from this table. This is done by putting stencils over the table, with holes placed over the desired positions. There are two stencils for each value of n , one for sines and one for cosines. The numbers chosen through the stencil are summed to give the desired quantities, $H_r(n)$, $H_i(n)$, $G_r(n)$, or $G_i(n)$. From these, $F_r(n)$ and $F_i(n)$ are calculated. Since $F_r(n) = F_r(-n)$ and $F_i(n) = -F_i(-n)$, the particle size line profile may be expressed as:

$$f(x) = F_r(0) + 2 \sum_1^{\infty} \left[F_r(n) \cos\left(\frac{2\pi nx}{a}\right) + F_i(n) \sin\left(\frac{2\pi nx}{a}\right) \right].$$

To interpret this line profile in terms of particle size, use has been made of the results of Warren and Averbach⁶. Two different average sizes may be calculated, either from the breadth of the line (d_β), or from the slope of a plot of $F_r(n)$ vs n at the origin (d_S).

The integral breadth of the line is given, in terms of the Fourier coefficients, by

$$\beta = \frac{\text{Area}}{\text{Maximum Amplitude}} = \frac{aF_r(0)}{F_r(0) + 2 \sum_1^{\infty} F_r(n)}$$

provided that the imaginary coefficients, $F_i(n)$, satisfy

$$\sum_1^{10} F_i(n) = 0$$

which was found to hold quite well experimentally. Then the particle size is:

$$d_{\beta} = \frac{0.94 \lambda}{\beta \cos \theta} \quad (2.3)$$

Warren and Averbach have shown that the average height of the column of "unit cells" perpendicular to the diffracting plane is

$$\bar{L} = \left(\frac{\partial F_r(n)}{\partial n} \right)_{n=0}^{-1}$$

while the "unit cell" dimension, a_3 , is given by

$$a_3 = \frac{\lambda}{a \cos \theta_0}$$

in which θ_0 is the Bragg angle at the peak of the line. The average particle size is then

$$d_s = \left(\frac{\partial F_r(n)}{\partial n} \right)_{n=0}^{-1} \cdot \frac{\lambda}{a \cos \theta_0}$$

2.2.3 Relation of XRD to Electron Microscope Particle Sizes

Bertaut¹³ has shown that d_β is given by

$$d_\beta = \frac{\iint M^2 d\xi_1 d\xi_2}{\iint M d\xi_1 d\xi_2}$$

in which ξ_1 and ξ_2 are spatial coordinates in the diffracting plane, and M is the particle dimension perpendicular to this plane. For spherical particles this reduces to

$$d_\beta = \frac{3}{4} \frac{\sum_i n_i d_i^4}{\sum_i n_i d_i^3} \quad (2.4)$$

where n_i is the number of particles in the particle size range with average diameter d_i .

Warren and Averbach⁶ have shown that d_s is given by

$$d_s = \frac{\iint M d\xi_1 d\xi_2}{\iint d\xi_1 d\xi_2}$$

which reduces in the same way, for spherical particles, to

$$d_s = \frac{2}{3} \frac{\sum_i n_i d_i^3}{\sum_i n_i d_i^2} \quad (2.5)$$

2.2.4 Errors, etc.

These measurements involve errors in reading, in computation, and in interpretation. In computing the particle size, using the Stokes technique, the curves are smoothed to a certain extent because the strips allow only integral amplitudes. The precision of the results cannot be expected to be better than about 8-10%.

In interpreting the shapes of the corrected line profiles in terms of particle size, several assumptions or uncertainties occurred. Line broadening can be caused by strain and stacking faults, as well as by small crystal size. Because of the limitations of the apparatus, it was not possible to distinguish definitely among these, and the assumption was made that all broadening was due to particle size. In comparing the X-ray results with those of the electron microscope, it was assumed that the particles were spherical. From the micrographs, most of the particles appear to be slightly ellipsoidal. Since, however, nothing is known of the relationship between the ellipsoidal and crystalline axes, there is no way to account for this departure, and the spherical assumption must be made. That it involves an error must be admitted. The constant 0.94 in equation 2.3 is uncertain to about 20%.¹⁴ This uncertainty probably

holds equally for all the powders here, and should therefore appear as a constant error.

One possible internal check upon the X-ray method can be obtained by comparing the two different particle sizes, d_p , and d_s , given by the method. In Table 2-1, the experimental values of d_p and d_s are compared to the appropriate averages calculated from the electron microscope distributions.

Table 2-1 - Comparison of X-ray and Electron Microscope Sizes

<u>Material</u>	<u>d_p, Å</u>	$\frac{3 \sum nd^4}{4 \sum nd^3}$ Å	<u>d_s, Å</u>	$\frac{2 \sum nd^3}{3 \sum nd^2}$ Å
Fe-8	389	370	323	224
Fe-7	282	406	212	233
Hyflux	213	329	147	272
NOL-1	207	254	140	201
NOL-2	228	171	178	143
Ugine	200	206	150	168

The first column lists the material; the second and third give values for d_p and the corresponding average sizes calculated from the electron microscope distributions, according to equation (2.4); the fourth and fifth give d_s and its counterpart average from equation (2.5). Serious discrepancies appear in d_p for Fe-7 and Hyflux, and in d_s for Fe-8 and Hyflux. For the rest, the X-ray and electron microscope data agree to within 40%. Considering the assumptions involved, this is reasonable agreement and indicates that the X-ray method is internally consistent.

Although it is a rigorous method for determining the part of the line profile due to the sample above, the Stokes-Fourier analysis method has not yet come into general use. Experimental work is still being published making use of Warren's⁵ older correction formula, or Jones⁹ curves. The data in Table 2-2 give a comparison among these three methods of computation.

Table 2-2 - Comparison of Warren, Jones, and Stokes Particle Sizes

<u>Material</u>	<u>d_p (Stokes)</u>	<u>Warren</u>	<u>Jones (b)</u>
Fe-8	389 Å	325 Å	425 Å
Fe-7	282	250	307
Hyflux	213	192	222
NOL-1	207	185	205
NOL-2	228	168	220
Ugine	200	165	183

These differences between the Stokes' method on the one hand and the Warren and the Jones' methods on the other are purely computational. They are in the same direction and of the same order as those found by Alexander and Klug¹⁴ for several other materials. Considering the simplicity to which the Patterson-Turcell strips have reduced the Fourier computations, it seems worthwhile to use the more objective Stokes method.

2.3 Surface Areas Measurements by the Nitrogen Adsorption Technique

2.3.1 Method

The adsorption of nitrogen gas on iron¹⁵ at liquid nitrogen temperatures follows an isotherm of the type II of Brunauer, etc.¹⁶

This type of isotherm can be represented by the equation developed by Brunauer, Emmett and Teller¹ (BET) in the relative pressure range $0.05 \leq P_A/P_0 \leq 0.35$. The equation may be written in the form

$$\frac{P_A}{V_A(P_0 - P_A)} = \frac{1}{V_M C} + \frac{C-1}{V_M C} \frac{P_A}{P_0}$$

in which P_A is the pressure at which V_A cc. of nitrogen, evaluated at STP, are adsorbed; P_0 is the vapor pressure of nitrogen at the measurement temperature; V_M is the STP volume necessary to cover the surface of the powder with a monolayer of nitrogen; C is a constant, which is given approximately by

$$C = e^{(E_1 - E_L)/RT}$$

and E_1 and E_L are, respectively, the average heat of adsorption in the first layer and the heat of vaporization of nitrogen.

The measurements were performed by determining the volume of nitrogen adsorbed at various pressures in the above pressure range with the sample immersed in a liquid nitrogen bath. The quantity $P_A/V_A(P_0 - P_A)$ was plotted as a function of P_A/P_0 , and the values for the constant C and V_M were determined from the slope and intercept of the resulting straight line. From the number of molecules contained in the volume V_M , the total surface area of the powder was calculated after choosing a value for the

area occupied by each nitrogen molecule. In this work Livingstone's¹⁷ value of 15.4 \AA^2 was used. The average diameter of the particles, d_N , was related to the total surface per gram, S , by the equation

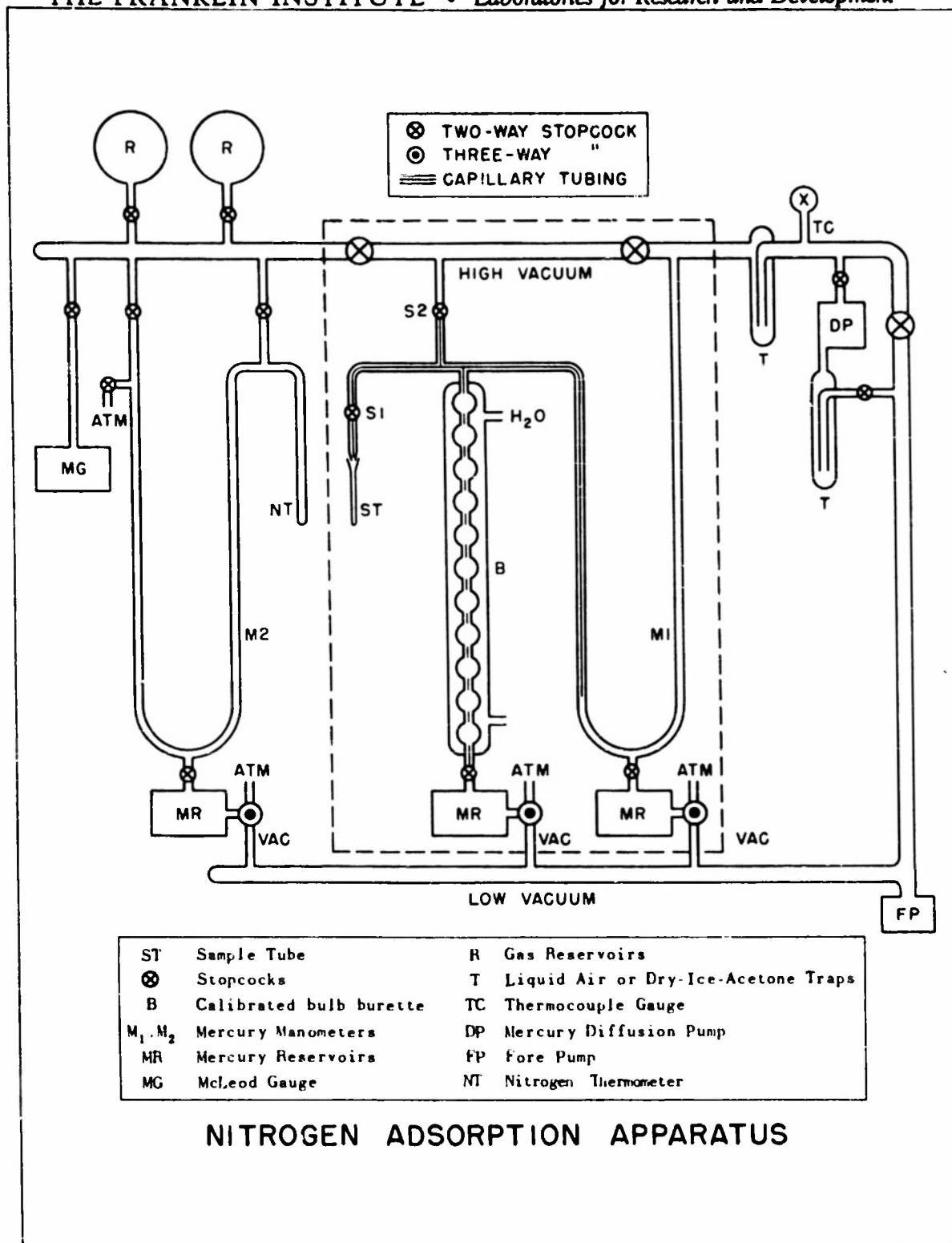
$$d_N = \frac{6}{\rho S}$$

in which ρ is the true density of the powder.

2.3.2 Apparatus

The apparatus used for these measurements was a standard volumetric apparatus, with many features similar to that used by the group at Lehigh University under Zettlemyer¹⁸. Figure 2-4 shows a schematic sketch of the apparatus. The heart of the apparatus is the region within the dotted square. ST is the sample tube; B a calibrated burette; M_1 a mercury manometer equipped with an electrical contact for setting purposes; NT a nitrogen thermometer, used to measure the bath temperature in terms of the vapor pressure of nitrogen (P_0); and M_2 a second mercury manometer used with the nitrogen thermometer. Associated with this apparatus are several gas reservoirs (R) for nitrogen and helium, a McLeod gage (MG), mercury reservoirs (MR), dry ice traps (T), mercury diffusion pump (D), and a mechanical forepump (FP).

The nitrogen used was Matheson prepurified, stated by the manufacturer to be 99.9% pure, which was passed through a drying tube containing Ascarite and Drierite, and over copper filings maintained at 500°C. The helium used for the measurement of the dead space was



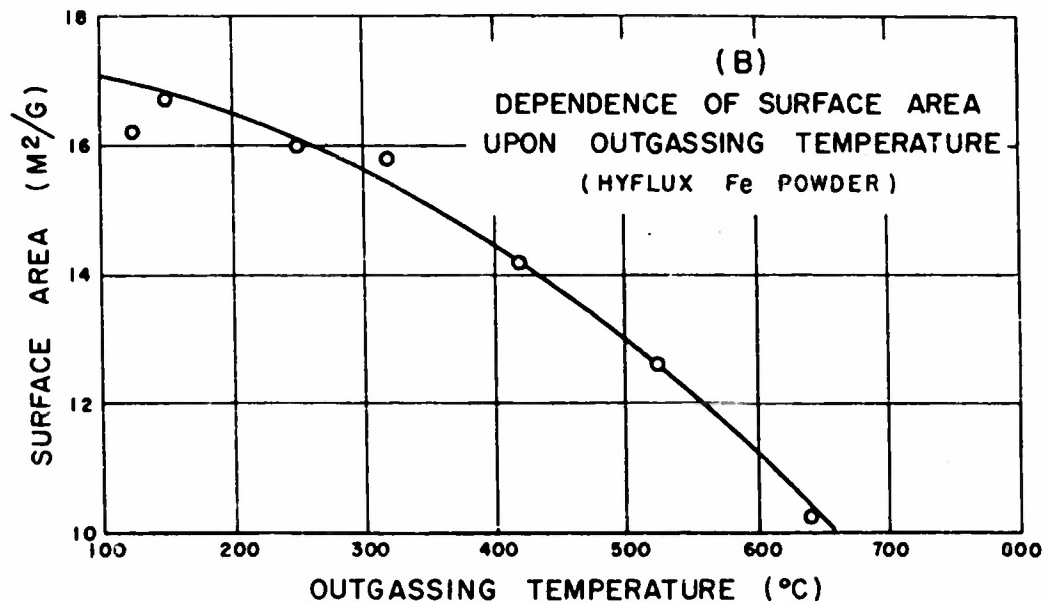
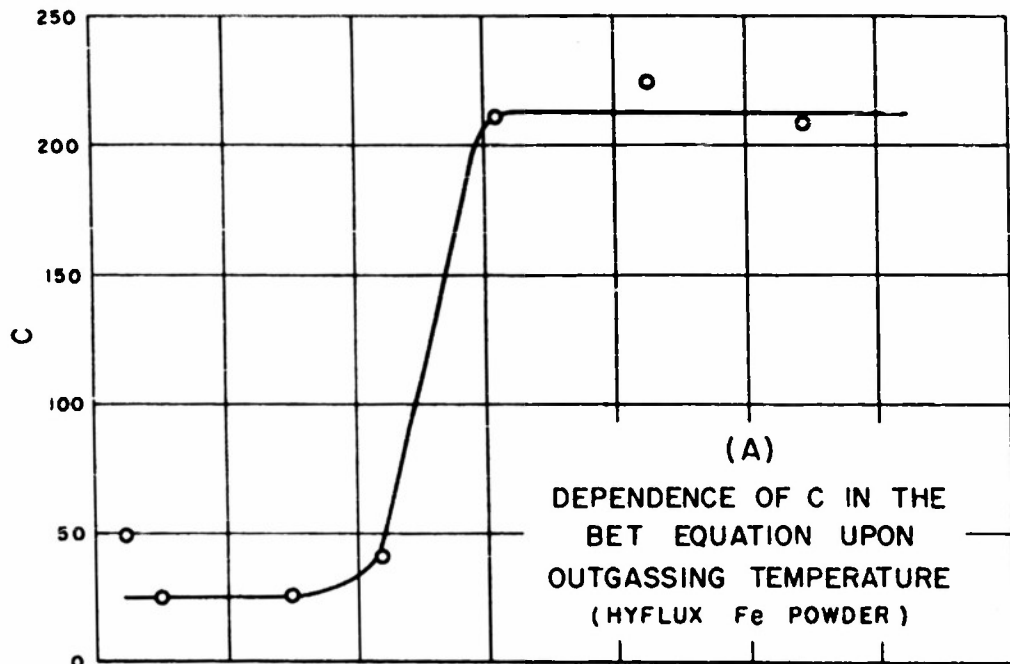
Matheson's helium 99.8% pure. It was used as supplied.

2.3.3 Conditions of Measurement

Outgassing of the sample and the system can be rather important in these measurements. The pressure during outgassing was less than one micron of mercury in the system. The sample was heated, usually for two and one-half to three and one-half hours at a temperature of approximately 200°C. The literature contains various recommended values of the outgassing temperature for iron, ranging from 110° (Emmett)¹⁹ to 450°C, given specifically for iron by Brunauer¹⁵, and Emmett and Brunauer²⁰. Since it is necessary during outgassing to avoid sintering, the outgassing temperature chosen must represent some sort of compromise between the outgassing and the sintering. Brunauer¹⁵ states that sintering of iron occurs at temperatures greater than 350°C, while chemisorbed hydrogen is probably not removed until the temperature is above 450°C. On the other hand, according to Emmett¹⁹, layers of chemisorbed hydrogen, oxygen, etc., probably do not interfere with the measurement.

In order to be completely certain of the proper outgassing temperature, a number of runs were made using Hyflux powder and several outgassing temperatures. All of the resultant isotherms gave good BET plots. Figure 2-5 shows the values of C and V_M calculated from these plots as a function of outgassing temperature. At about 350°C, C rose sharply from very low values to about 220, which may be compared to the value given by Brunauer¹⁵ for the identical system, $C = 230$. This sharp rise with

EFFECT OF OUTGASSING TEMPERATURE UPON THE ADSORPTION ISOTHERMS



increasing outgassing temperature is the behavior to be expected from the definition of C. Thermodynamics shows that a chemisorbed layer tends to lower the free surface energy of the powder. This in turn lowers the heat of adsorption of the first physically adsorbed layer of nitrogen. $E_1 - E_L$ is therefore smaller where a chemisorbed layer persists, at the lower outgassing temperatures. As this chemisorbed layer is pumped off, $E_1 - E_L$ should rise, and with it C.

At the same time that this sharp rise in C occurs, V_M showed only a slow smooth drop with no discontinuous change. It is highly probable that the slow drop in V_M was simply due to sintering. Therefore, V_M as determined with outgassing temperatures lower than 350°C is probably valid, confirming Emmett's statement. For this reason the final outgassing conditions chosen were 200°C and two and one-half hours to three and one-half hours.

2.3.4 Measurement Procedure

When the measurement was made, the powder sample was loaded into the sample tube, which was then packed with glass wool to prevent escape of the light powder during outgassing. Tests showed no measurable adsorption on the glass wool. The system and sample were evacuated, outgassed, and cooled. A liquid nitrogen bath in a dewar was applied to both the cell and the nitrogen thermometer. Nitrogen was admitted to the nitrogen thermometer at a pressure greater than P_0 , which was about atmospheric. Some of this nitrogen, therefore, condensed in the thermometer,

giving a reservoir of liquid nitrogen and insuring that the pressures measured corresponded to the saturation pressure of nitrogen at the bath temperature. The actual bath temperature was calculated from these pressures using the data of Loebenstein and Dietz.²¹

The system volume, which was from 5 to 10 cc, is enclosed by stopcocks S_1 and S_2 , by burette B, and by the manometer M_1 , (Figure 2-4), and was measured with helium. Helium was admitted to the system with the mercury in the burette at a low level, the system was sealed off, and then the mercury was raised in the burette bulb by bulb, and the pressure registered on M_1 measured with a cathotometer. Since the total amount of gas in the system was constant, and since at room temperature helium acts like a perfect gas, these pressures and volumes were related by the equation

$$PV_B = (P' - P) V_S .$$

P' is the pressure with the manometer completely full of mercury, V_{B_0} is the volume of the manometer occupied by gas, and V_S is the system volume. By plotting PV_B against P , a straight line was obtained whose slope was $-V_S$.

The dead space, which was the space not occupied by powder in the cell below stopcock S_1 , was measured in approximately the same fashion. Although the temperature of this dead space was that of a liquid nitrogen bath, for convenience the dead-space volume was usually expressed in equivalent cc of gas at STP. Its magnitude was 2 to 3 cc. In this case,

helium was admitted to the system with the cell closed and the pressure P_1 noted. Then the cell was opened and the pressure P_2 again noted. Using the perfect gas law, and the condition that the total amount of gas in the system remained constant, these pressures and volumes were related by the equation

$$\frac{P_1 V_S}{T_R} = \frac{P_2 V_S}{T_R} + \frac{P_2 V_D}{T_A}$$

in which T_R is room temperature, T_A the bath temperature, and V_D the actual volume of the dead space. From this equation the dead-space volume could be calculated. Nitrogen does not obey the ideal gas laws; therefore this dead space volume was corrected, following Emmett¹⁹, by a factor of 1.05 to account for the non-ideality of nitrogen at 77°K.

Adsorption was measured by admitting nitrogen to the evacuated system with the cell closed, and noting the pressure P_1 and the total system volume, V_{BI} plus V_S . The cell was then opened, allowed to come to equilibrium, and the pressure remeasured. The mercury in the burette was raised bulb by bulb and the pressure noted in the system at the end of each step. At the beginning of the run it was necessary to wait 10 to 20 minutes for equilibrium, At higher pressures, a smaller wait was required.

The volume adsorbed, reduced to STP was calculated from equation

$$V_A = \frac{T_S}{P_S} \left[\frac{P_1(V_S + V_{B1})}{T_R} - \frac{P_A(V_S + V_{BA})}{T_R} - \frac{P_A V_D}{T_A} \right]$$

V_A is the total volume adsorbed converted to STP from the beginning of the run up to the given step; P_A is the system pressure for this step; T_S and P_S are standard temperature and pressure; V_{B1} and P_1 are the initial burette volume and system pressure before opening the cell, V_{BA} the burette reading corresponding to this particular step, and T_R and T_A room temperature and the temperature of the adsorption cell respectively. The quantities P_A , and V_A , calculated from this equation, were then introduced into the BET equation and V_M obtained as described above.

2.3.5 Errors

An estimated error in V_A of about 0.033 cc was calculated. V_M and C were derived from the data by the least squares method, with estimated errors of about 1% in V_M . The same error should be reflected in the value for the total surface. The figures in Table 2-3 show a comparison between runs made on several powders under identical conditions.

Table 2-3 Reproducibility of Surface Area Measurements

Run No.	Material	Surface Area M ² /g
20	NOL-1	23.09
21	"	24.40
22	"	23.68
23	"	23.68
25	Hyflux	16.18
40	"	15.79

The deviations are somewhat greater than this estimated error but of the same order of magnitude. The actual random errors should be taken as those shown in the table.

Beside the random errors there are absolute errors involved in the measurement. These include uncertainties in the purity of the gases, completeness of outgassing, and the occurrence of sintering. These are errors very hard to estimate. In addition, there are errors inherent in the theory. One of these is involved in the choice of the area occupied by each nitrogen molecule. This choice may be in error by as much as 5%, judging from the data of Livingstone¹⁷, and others. (15, 18, 22, 23, 24) Beeck²⁵ has shown that because of the high heat of adsorption on metals, N₂ may be quasi-chemisorbed to the extent of a half monolayer at 77°K at pressures less than 0.1 millimeter of mercury. A complete monolayer will then be laid down on top of this chemisorbed layer in the pressure range $0.05 \leq P_A/P_0 \leq 0.35$, which in this case includes the range from 38 to 230 millimeters of mercury. The measurements will therefore appear to give a normal BET curve, but enough nitrogen will have been adsorbed for one and one-half monolayers. The measured V_M may therefore be greater than

the true value by a factor of 1.5, which would make the experimental particle size lower than the true value by 1.5.

This behavior shown by Beeck's work is true for clean iron surfaces, for which the heat of adsorption of nitrogen ranges from 10,000 to 5,000 calories per mole. Beeck's surfaces were evaporated films and were undoubtedly very clean. Our surfaces, with only mild outgassing, are undoubtedly quite dirty. Our C values indicate that the heat of adsorption of nitrogen on our surfaces was less than 2,000 calories per mole, so that it is probably unlikely that any ~~farther~~ amount of chemisorption took place on our surfaces. It is therefore probable that our surface areas are not in error by anything like the 1.5 factor due to this cause, although an uncertainty remains. We plan in the near future to repeat ~~some~~ of these measurements with methane, which has been shown by Beeck not to be chemisorbed.

If the surface of the particles is not perfectly smooth, then a larger surface area will be measured by this method than corresponds to the actual particle diameter. The effect would be to make the particle sizes calculated from the surface area smaller than their true value.

In the packing of particles together, the points on the surface where the particles touch are inaccessible to the nitrogen molecules. This would have the effect of making the measured surface lower than the true surface, and the measured diameter larger than the true diameter. A simple calculation shows that, for perfect spheres of about 300 Å diameter in closest packing, a 10 percent error would be involved. This

figure represents a maximum, since nothing like closest packing is to be expected in a real powder.

There seems to be a tendency for these absolute errors to oppose each other. Sintering and ~~packing~~ packing will make the measured particle size larger than the true value, while the result of roughness and chemisorption will be the reverse. The actual effects cannot be evaluated; thus, a rather large uncertainty, of the order of 50 percent, must be admitted in the absolute values of the particle sizes.

2.3.6 Relation of N_2 Adsorption to Electron Microscope Diameters

In order to compare the nitrogen adsorption data with the distribution determined by the electron microscope, it is necessary to determine what sort of average particle size is measured by the surface area method. The average particle diameter is calculated using the equation

$$d = \frac{6}{\rho S} = \frac{6W}{\rho A}$$

in which A is the total surface area of the sample, W is its weight, S is the surface area/g, and ρ is the true density. In terms of the individual particles, W can be given by

$$W = \rho \sum_i n_i \left(\frac{\pi d_i^3}{6} \right)$$

and A by

$$A = \sum_i n_i (\pi d_i^2) .$$

Then the average particle size determined by this method is

$$d_N = \frac{\sum_i n_i d_i^3}{\sum_i n_i d_i^2}$$

in which d_i is the diameter of the particles of the i^{th} particle size range.

2.4

True Powder Density

The true powder densities were determined with the nitrogen adsorption apparatus by measuring, with helium at room temperature, the cell volume with and without a weighed amount of powder. The technique of measuring this cell volume was identical to that used measuring the system volume, as described above. Because of the small amount of material available in most cases, the volume of the powder measured was of the order of 0.1-0.2 cm³, and a precision better than 7% cannot be claimed.

3. CONCLUSION

3.1 Results

The electron microscope gave complete particle size distributions whereas the other two methods gave different, specific averages.* In order to compare the three methods, expected values for these averages were calculated from the microscope distributions. In Figure 3-1, these expected values are plotted as abscissae and the experimental values are plotted as ordinates. If perfect agreement were obtained between each method and the microscope, these data would fall on the 45° lines. The X-ray sizes are all d_{β} .

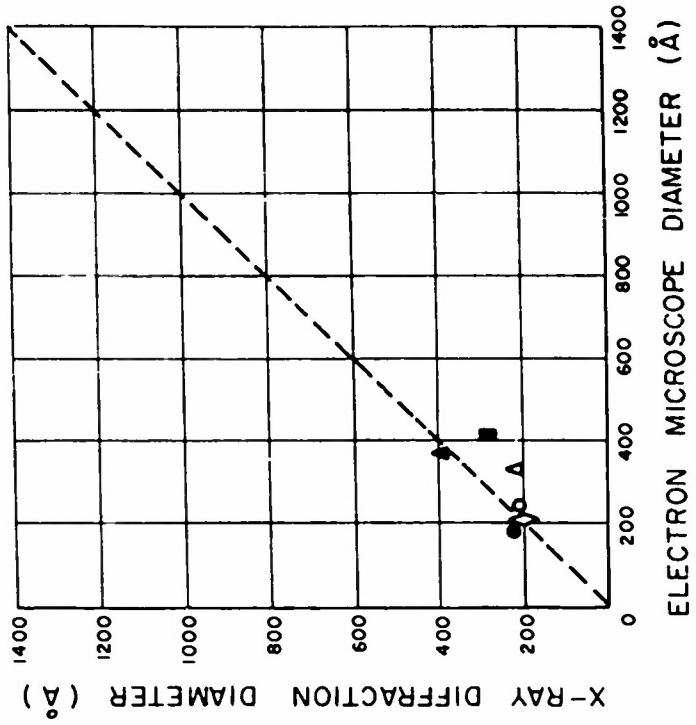
3.2 Discussion

Reasonably good agreement is in fact obtained between the X-ray diffraction method and the electron microscope; the N₂ adsorption sizes, on the other hand, are always high. Several of the effects discussed in section 2.3.5 might have caused the N₂ adsorption values to be high, including the packing error and the choice of the area occupied by each N₂ molecule. For the latter, both 16.2 Å²(15, 22, 23, 24), and 15.4 Å²(17, 18) have been suggested. Use of the former rather than the latter would reduce the N₂ sizes found in this study by about 5%.

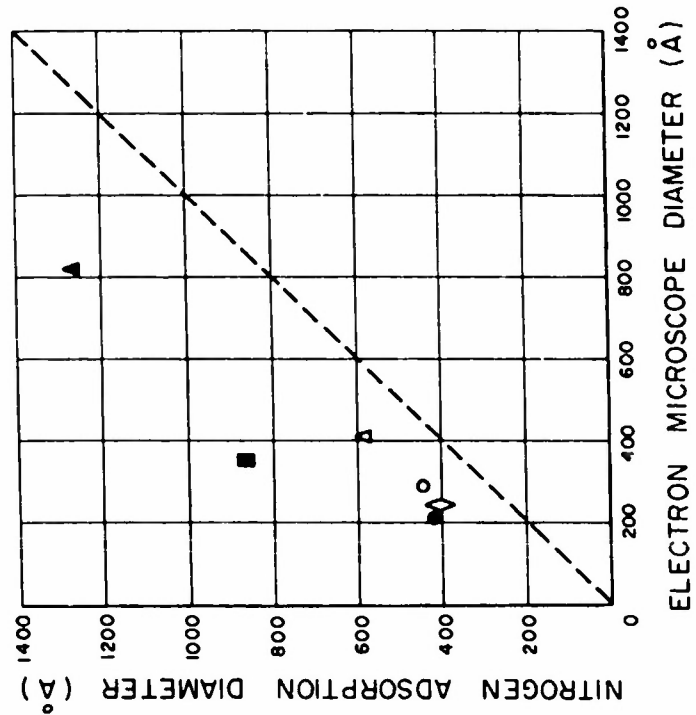
* Under favorable experimental conditions, the pure X-ray diffraction line profile can be interpreted to give the complete particle size distribution. (6, 13) The required conditions are more rigorous than could be achieved here, and only the two averages described above, d_{β} and d_s , were obtained.

COMPARISON OF MEASUREMENTS OF IRON POWDERS

(B) X-RAY DIFFRACTION



(A) NITROGEN ADSORPTION



The presence of appreciable amounts of oxide in the powders, as indicated by Table 1-1, may also have made the N_2 size larger than the others. The X-ray method must have responded only to the metallic part of the sample, since an Fe diffraction line was used. The agreement between the X-ray and electron microscope methods indicates that the latter also gave only the size of the Fe component. Hence, if appreciable oxide layers were present on the particles, surface measurements would give particle sizes larger than the purely Fe part. There is, however, no correlation to be seen between oxide content and the discrepancy between the N_2 adsorption sizes as compared to the others.

The following conclusions are drawn from this work:

(1) If sufficient care be taken to produce good dispersions, the electron microscope may be used to determine reliable particle size distributions of metallic single-domain powders.

(2) For single-domain ferromagnetic particles, these dispersions may be obtained by magnetic dispersion, as discussed in section 2.1.1 of this report.

(3) These electron microscope distributions must be compared to the average sizes obtained from one or two independent methods. Not only is this necessary to be sure that the microscope specimens truly represent the whole sample, but also it helps at times to decide whether large objects in the micrographs are single particles or are clumps.

(4) For this purpose, the X-ray method is the better of the two used here, since it measures the same part of the sample as the electron microscope.

(5) Quite often, skew distributions are found with these powders. For this reason, only a method giving the complete distribution is of real value. The other methods give only particular averages, which may be quite unlike the one desired in using the data. The electron microscope must be used, then, to give data that are truly significant.

Alan D. Franklin


Project Leader

Since this investigation is still in progress, the conclusions expressed in this report are tentative.

REFERENCES

1. S. Brunauer, P. Emmett, and E. Teller, *JACS* 60, 309 (1938).
2. P. Debye, "Polar Molecules", Chemical Catalog Co., N. Y. (1929).
3. J. Watson and W. Grube, *J. Appl. Phys.* 23, 793 (1952).
4. W. H. Meiklejohn and T. O. Paine, ONR Conference on Magnetism, Washington, D. C., (1952).
5. B. E. Warren, *J. Appl. Phys.* 12, 375 (1941).
6. B. E. Warren and L. Averbach, *J. Appl. Phys.* 21, 595 (1950).
7. W. C. Ellis and E. S. Greiner, *Trans. Am. Soc. Metals* 29, 415 (1941).
8. R. W. James, "The Optical Principles of the Diffraction of X-rays" p. 536, G. Bell and Sons, London, (1948).
9. F. W. Jones, *Proc. Roy. Soc.* 166A, 16 (1938).
10. L. Alexander, *J. Appl. Phys.* 19, 1068 (1948); 21, 126 (1950).
11. A. R. Stokes, *Proc. Roy. Soc.* 61, 382 (1948).
12. A. L. Patterson and G. Tunell, *J. Mineral. Soc. Am.* 27, 655 (1942).
13. F. Bertaut, *Acta Cryst.* 3, 14 (1950).
14. L. Alexander and H. P. Klug, *J. Appl. Phys.* 21, 137 (1950).
15. S. Brunauer, "Physical Adsorption", Princeton (1943).
16. S. Brunauer, L. S. Deming, W. E. Deming and E. Teller, *JACS* 62, 1723 (1940).
17. H. K. Livingstone, *J. Colloid Sci* 4, 447 (1949).
18. W. C. Walker, Ph.D. Thesis, Lehigh University.
19. P. H. Emmett, "Symposium on New Methods for Particle Size Determination in the Subsieve Range", ASTM (1941).

20. P. H. Emmett and S. Brunauer, JACS 56, 35 (1934).
21. W. V. Loebenstein and V. R. Dietz, J. Res. Natl. Bur. Stds. 46,
51 (1951).
22. H. L. Pickering and H. C. Eckstrom, JACS 74, 4775-7 (1952).
23. M. L. Corrin, ACS 23, 4061 (1951).
24. W. D. Harkins and G. Jura, J. Chem. Phys. 11, 431 (1943).
25. O. Beeck, in "Advances in Catalysis" Vol II, p. 155, Academic
Press, N. Y. (1950).